



Cite this: *Environ. Sci.: Nano*, 2025, 12, 2008

## Physiological and transcriptomic responses of *Chlorella vulgaris* to novel antibacterial nanoparticles of ethyl cyanoacrylate polymer†

Di Zhang,‡<sup>a</sup> Keqing Liu,‡<sup>a</sup> Chengcheng Feng,‡<sup>a</sup> Xianmin Wang,<sup>a</sup> Ayat J. S. Al-Azab,<sup>b</sup> Han Lu,<sup>a</sup> Haiyan Ma,<sup>c</sup> Ying Tang,<sup>a</sup> Li Xu,<sup>a</sup> Takeshi Ohama <sup>d</sup> and Fantao Kong <sup>\*a</sup>

Ethyl cyanoacrylate nanoparticles (ECA-NPs) have recently been reported as promising novel antibacterial NPs capable of inhibiting the growth of several Gram-positive and Gram-negative bacteria. However, the effects of ECA-NPs on microalgae, which are primary producers in aquatic ecosystems, remain unknown. In this study, we examined the effects of ECA-NPs on the microalga *Chlorella vulgaris* (*Chlorella*) at both cellular and molecular levels. A high concentration of ECA-NPs (100  $\mu\text{g mL}^{-1}$ ) exhibited strong growth inhibitory effects on *Chlorella*. In the ECA-NP-treated cells, transmission electron microscope (TEM) observations showed the prominent internalization of ECA-NPs in the periplasmic space and vacuoles. Moreover, notable morphological changes such as a thinner cell wall, stacked thylakoid structure, and plasmolysis were observed. ECA-NP exposed *Chlorella* secreted more extracellular polymeric substances (EPS) and accumulated more storage lipids (mainly triacylglycerol, TAG) compared to the control. However, the contents of total fatty acids and starch were decreased, and photosynthetic activity was reduced. In addition, the content of intracellular reactive oxygen species (ROS) and the activities of antioxidant enzymes in ECA-NP-treated cells were significantly higher than those in the control. Transcriptomic analysis revealed the downregulation of genes that are involved in the drug binding/catabolic process, chemical stimulus detection, and cell wall component catabolic process (chitin catabolism), while genes involved in the photosynthetic membrane and plastid thylakoid were upregulated. These results indicated that the effects of ECA-NP exposure are not limited to specific metabolic pathways, but rather influence metabolic pathways across the entire cell. This study also provided new insights into the potential toxic effects associated with cyanoacrylate NPs in phytoplankton.

Received 13th September 2024,  
Accepted 20th January 2025

DOI: 10.1039/d4en00861h

rsc.li/es-nano

### Environmental significance

The expanding applications of engineered nanoparticles (NPs) in medical and industrial fields have resulted in increased exposure of phytoplankton to various NPs. Recently, biodegradable ethyl cyanoacrylate nanoparticles (ECA-NPs) have been reported as promising novel antibacterial agents. However, the effects of ECA-NPs on microalgae, primary producers in aquatic ecosystems, remain unknown. We found that high concentrations of ECA-NPs induce changes in cell morphology and photosynthetic activity, leading to increased ROS generation, which results in transcriptomic and metabolic alterations. The effects of ECA-NP exposure are not limited to specific metabolic pathways, but rather influence metabolic pathways across the entire cell. To the best of our knowledge, this is the first report to elucidate the mechanisms by which novel antibacterial nanoparticles of ethyl cyanoacrylate polymer affect aquatic phytoplankton.

<sup>a</sup> MOE Key Laboratory of Bio-Intelligent Manufacturing, School of Bioengineering, Dalian University of Technology, Dalian, 116024, Liaoning, China.

E-mail: kongfantao@dlut.edu.cn; Tel: +86 15642336188

<sup>b</sup> Department of Biotechnology and Genetic Engineering, Faculty of Science, Philadelphia University, Amman, Jordan

<sup>c</sup> Institute of Hydrobiology, Chinese Academy of Sciences, Wuhan, Hubei 430072, China

<sup>d</sup> School of Environmental Science and Engineering, Kochi University of Technology, 185 Miyakuchi, Tosayamada, Kami-City 782-8502, Japan

† Electronic supplementary information (ESI) available. See DOI: <https://doi.org/10.1039/d4en00861h>

‡ These authors contributed equally to this work.

### Introduction

Antibiotics are widely used to prevent bacterial and fungal infections in both humans and animals, leading to an increase in global antibiotic consumption.<sup>1</sup> However, antibiotic-resistant bacterial infections and multi-drug-resistant ‘superbugs’ are on the rise due to the overuse of these medications.<sup>2</sup> The relatively low biodegradability of antibiotics means that most residual compounds enter aquatic environments, raising concerns about their toxic effects on microalgae.<sup>3</sup> Microalgae, which are

photosynthetic microorganisms found in various aquatic habitats, serve as primary producers in these ecosystems.<sup>4,5</sup> Although microalgae have shown potential in removing antibiotics (e.g., metronidazole), microplastics (e.g., polystyrene), and toxic dyes (e.g., alizarin red S) from synthetic solutions, further investigation is necessary to fully understand the underlying mechanisms.<sup>6-8</sup> Moreover, residual antibiotics in aquatic environments can alter the physiological characteristics of microalgae, impair primary production, and threaten the overall health of the ecosystem.<sup>9</sup> Therefore, developing novel and effective antibiotic alternatives is crucial to combat antibiotic resistance in bacteria.

Recently, several nanoparticles (NPs) and their derivatives have been reported to exhibit antibacterial activity, making them potentially useful for medical applications.<sup>10</sup> Traditional metal NPs, such as silver NPs (Ag-NPs), have been widely employed. However, Ag-NPs have potentially harmful effects on human health.<sup>11</sup> In contrast, polycyanoacrylate NPs (PCA-NPs) are commonly biodegradable and show no prominent toxic effects in animals.<sup>12</sup> PCA-NPs are mostly used to produce adhesives, surgical glue, and drug carrying nanocapsules,<sup>13-15</sup> and have also been reported as potential antibiotic alternatives against bacteria.<sup>16,17</sup> For example, the engineered poly(isobutyl cyanoacrylate) resin NPs (iBCA-NPs) can inhibit the growth of a broad spectrum of microalgae, such as *Chlamydomonas reinhardtii*, *Chattonella marina*, *Prymnesium parvum*, *Thalassionema nitzschiooides*, *Heterocapsa triquetra* and *Rhodomonas atrorosea*, likely due to damaged cell walls and increased reactive oxygen species (ROS) generation.<sup>18,19</sup> In addition, iBCA-NPs can induce the production of more energy reserves (e.g., triacylglycerols and starch) compared to previously reported NPs, probably due to increased ROS content, enhanced antioxidant enzyme activities, and upregulated expressions of key genes involved in triacylglycerol and starch biosynthesis.<sup>20</sup>

We recently reported that engineered ethyl cyanoacrylate nanoparticles (ECA-NPs) are promising novel antibacterial agents capable of inhibiting the growth of Gram-positive and Gram-negative bacteria.<sup>17</sup> ECA-NPs showed the highest growth inhibitory effect on bacteria compared to other tested PCA-NPs, including iBCA-NPs and ethoxyethyl cyanoacrylate NPs.<sup>17</sup> It is reported that exposure to ECA-NPs induces different physiological responses in Gram-positive and Gram-negative bacteria. In *E. coli*, apoptosis-like death is induced by ROS generation due to the presence of ECA-NPs, while ECA-NP-treated *B. subtilis* cells undergo necrosis instead of apoptosis.<sup>21</sup> However, the underlying molecular mechanisms remain unknown.

The eukaryotic green microalga *Chlorella vulgaris* (hereafter *Chlorella*) is widely distributed in the aquatic environment and is commonly used as a model microorganism in toxicity assays. *Chlorella* has been utilized for the elimination of tetracycline and for studying the toxic effects of microplastics in aquatic environments.<sup>22,23</sup> It is also utilized as a dietary supplement and a protein-rich food additive, serving as a promising platform for the commercial production of valuable

macromolecules.<sup>24</sup> In addition, *Chlorella* has emerged as a potential microorganism for bioremediation studies aimed at mitigating environmental pollution.<sup>25</sup> It is effective in removing a variety of pollutants, including inorganic nutrients, heavy metals, fertilizers, pharmaceuticals and other emerging pollutants from wastewater and effluents.<sup>24-26</sup>

In this study, *Chlorella* was utilized as a model organism to investigate the physiological and biochemical responses to novel antibacterial ECA-NPs. Transcriptome analysis was also conducted to elucidate the underlying molecular responses. To the best of our knowledge, this is the first report examining the effects of antibacterial cyanoacrylate nanoparticles on microalgae, and potential underlying mechanisms have also been proposed.

## Results

### Effects of ECA-NPs on cell growth and morphology of *Chlorella*

To assess the impact of ECA-NPs, which had a mean size was  $82.5 \pm 0.42$  nm and zeta potential of  $6.72 \pm 2.78$  mV, on the growth of *Chlorella*, cell growth kinetics were examined in culture media supplemented with varying concentrations of ECA-NPs. The results showed that the cell growth kinetics of *Chlorella* treated with  $50 \mu\text{g mL}^{-1}$  ECA-NPs were not significantly different from those of the control (Fig. 1A), however, exposure to  $100 \mu\text{g mL}^{-1}$  ECA-NPs resulted in a significant delay ( $p \leq 0.01$ ). Furthermore, treatment with  $200 \mu\text{g mL}^{-1}$  ECA-NPs led to further growth inhibition and arrested cell development (Fig. 1A) ( $p \leq 0.01$ ). These results indicated that relatively low concentrations of ECA-NPs do not significantly alter cell growth, while higher concentrations of ECA-NPs resulted in retarded growth. Due to the arrested cell growth observed at  $200 \mu\text{g mL}^{-1}$  ECA-NPs, the physiological response at this concentration was not examined in this study.

Morphological and structural characterization of *Chlorella* cells was conducted using a transmission electron microscope (TEM) after exposure to  $100 \mu\text{g mL}^{-1}$  ECA-NPs for three days. In the non-exposed cells used as controls, TEM images exhibited thick cell walls surrounding the entire cell periphery and thylakoid membrane structures (Fig. 1B). However, after 3 days exposure to ECA-NPs at  $100 \mu\text{g mL}^{-1}$ , the cells exhibited irregular cellular morphology, such as a thinner cell wall and stacked thylakoid structures as well as the occurrence of plasmolysis (Fig. 1B). ECA-NPs primarily accumulated at the interface between the cell wall and plasma membrane (periplasmic space). In addition, ECA-NPs and their aggregates were also observed at inside of the vacuoles, cytosol and chloroplast (Fig. S1†), indicating that the ECA-NPs penetrated into the cell by overcoming the thinned cell wall or through areas where the cell wall had disappeared.

### The changes of EPS after exposure to ECA-NPs

To examine changes in extracellular polymeric substances (EPS), which are crucial for self-defense against external stimuli,<sup>27</sup> the time course of EPS content and production in



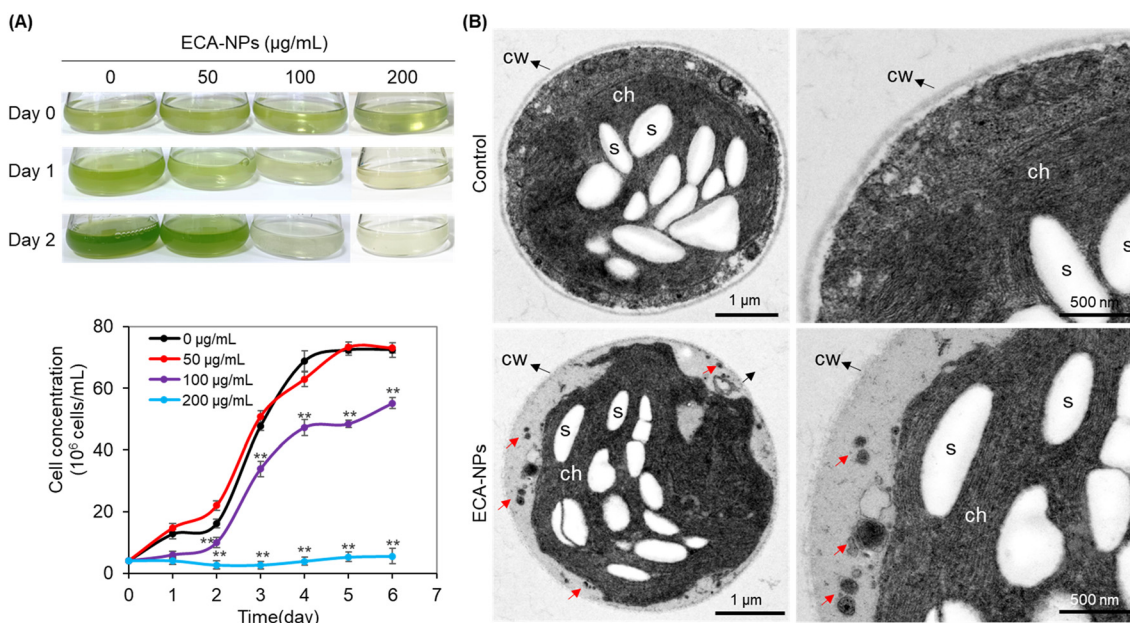


**Fig. 1** Effects of ECA-NPs on the growth and morphology of *Chlorella vulgaris*. (A) The cell growth in culture media containing different concentrations of ECA-NPs. (B) The morphological changes of the cells exposed to ECA-NPs observed by transmission electron microscopy (TEM). The cells were exposed to ECA-NPs ( $100 \mu\text{g mL}^{-1}$ ) for 3 days. CW, cell wall; Ch, chloroplast; S, starch. The red arrows indicate the ECA-NPs. Statistical analysis was conducted using Student's *t*-test (\*\* $p \leq 0.01$ ).

*Chlorella* was evaluated under varying concentrations of ECA-NP exposure. The results indicated that EPS content and production in the culture medium of all the ECA-NP treated (50 or 100  $\mu\text{g mL}^{-1}$  of ECA-NPs for one, two, or three days) *Chlorella* increased compared to the untreated control (Fig. 2). Furthermore, EPS content was significantly higher at 100  $\mu\text{g mL}^{-1}$  than at 50  $\mu\text{g mL}^{-1}$  (Fig. 2A) ( $p \leq 0.01$ ). When *Chlorella* was exposed to 100  $\mu\text{g mL}^{-1}$  ECA-NPs for three days, EPS content and production were 3.2 mg  $\text{g}^{-1}$  dry cell weight (DCW) and 1.9-fold higher than those of the untreated control, respectively (Fig. 2A and B). These results indicated that exposure to ECA-NPs stimulates EPS production, with the effect positively correlating with ECA-NP concentration.

The increased EPS production following ECA-NP treatment may be attributed to the enhanced internalization of ECA-NPs.

#### The changes of carbon reserves after exposure to ECA-NPs

The impact of ECA-NPs on the production of storage oils (triacylglycerols, TAG) in *Chlorella* was examined. The results showed that cellular TAG content and production were significantly increased in *Chlorella* exposed to ECA-NPs (Fig. 3A–C). In 100  $\mu\text{g mL}^{-1}$  ECA-NP-treated *Chlorella* cells, the TAG content and production were 11.7  $\mu\text{g mg}^{-1}$  and 4.1  $\mu\text{g mL}^{-1}$ , which were increased by 4.7 and 3.3-fold compared

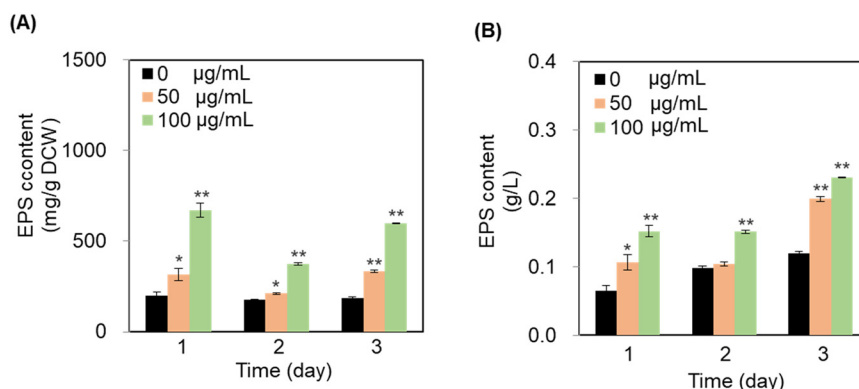


**Fig. 2** The dynamic changes of EPS content in ECA-NPs-treated *Chlorella vulgaris*. (A and B) EPS content and production of the cells following exposure to different concentrations of ECA-NPs, respectively. The cells were cultivated under different concentrations of ECA-NPs and the EPS was harvested and examined at the indicated day. EPS, extracellular polymeric substances. DCW, dry cell weight. Statistical analysis was conducted using Student's *t*-test (\* $p \leq 0.05$ , \*\* $p \leq 0.01$ ).



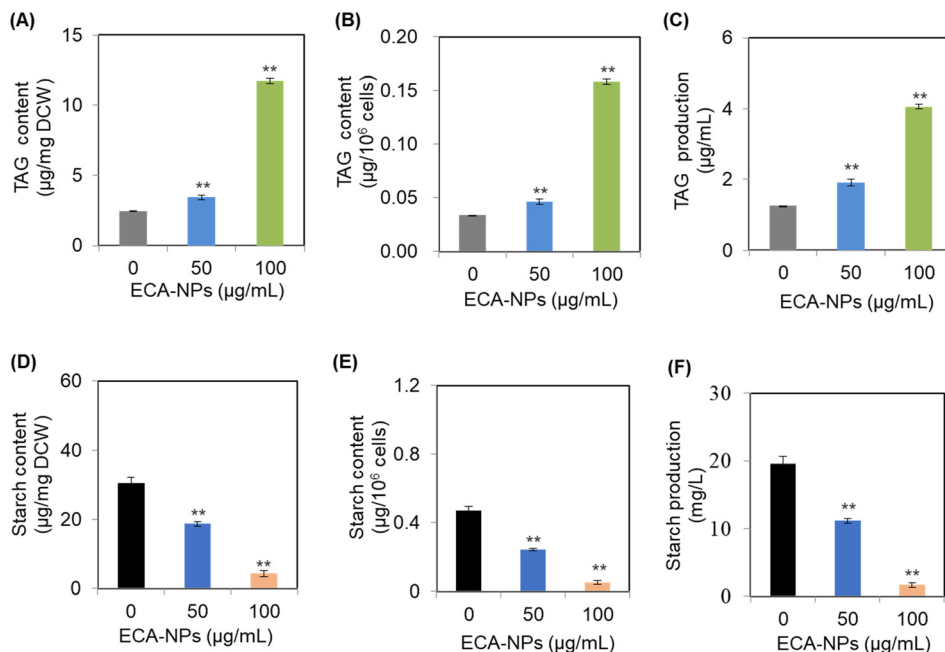


**Fig. 3** The impact of ECA-NPs on the production of triacylglycerols (TAG) and starch accumulation in *Chlorella vulgaris*. (A–C) TAG content and production of the cells following exposure to different concentrations of ECA-NPs, respectively. DCW, dry cell weight. (D–F) Starch content and production of the cells following exposure to different concentrations of ECA-NPs. The cells were collected for analysis following a three-day treatment with ECA-NPs. Statistical analysis was conducted using Student's t-test (\*\* $p \leq 0.01$ ).

with those in untreated control, respectively (Fig. 3A and C). These results indicated that exposure to ECA-NPs enhanced TAG accumulation and production. Starch serves as another primary intracellular energy reserve in microalgae.<sup>28</sup> Therefore, the starch content in the ECA-NP-treated cells was also analyzed. In 100  $\mu\text{g mL}^{-1}$  ECA-NP-treated *Chlorella* cells, the starch content and production were 4.3  $\mu\text{g mg}^{-1}$  and 1.7  $\text{mg mL}^{-1}$ , which was decreased by 86% and 92% compared with that in untreated control, respectively (Fig. 3D and F). These results indicated that exposure to ECA-NPs promoted TAG production but compromised starch production. The enhanced carbon flux towards TAG synthesis appears to have negatively impacted starch synthesis in the ECA-NP treated cells.

#### Total fatty acid analysis after exposure to ECA-NPs

The influence of ECA-NP exposure on the total fatty acid (TFA) content and composition was further examined to determine how these nanoparticles affect the lipid metabolism and fatty acid profile of *Chlorella*. The results showed that TFA content and production decreased in *Chlorella* after exposure to different concentrations of ECA-NPs compared to the control (Fig. 4A–C). In ECA-NP-treated *Chlorella* cells, TFA production was reduced by up to 39% compared to the control (Fig. 4C). TFA profile analysis revealed a decrease in the ratio of C16:0 and an increase in C18:3(9,12,15) in the ECA-NP-treated cells, while the ratios of other fatty acids in TFA remained unchanged compared to the control (Fig. 4D). These results suggest that ECA-NPs

treatment led to alterations in TFA levels and fatty acid composition, highlighting the potential impact of ECA-NPs on lipid metabolism in microalgae. Additionally, the findings may provide insights into the mechanisms by which ECA-NPs influence cellular processes and overall fitness in microalgae.

#### Oxidative damages after exposure to ECA-NPs

To evaluate the oxidative stress in *Chlorella* after exposure to ECA-NPs, the reactive oxygen species (ROS) content and the activities of antioxidant enzymes were examined. The results indicated that the ROS content in ECA-NP-exposed cells increased, with levels in ECA-NP-treated cells reaching up to 3.4-fold higher than those in the control (Fig. 5A). Moreover, the activities of antioxidant enzymes, such as superoxide dismutase (SOD) and malondialdehyde (MDA), were significantly enhanced (>17-fold) in cells treated with 100  $\mu\text{g mL}^{-1}$  ECA-NPs (Fig. 5B and C). The results indicated that exposure to ECA-NPs triggered more ROS generation, which may lead to increased activities of antioxidant enzymes to mitigate cytotoxic effects caused by oxidative damages.

To know the effects of ECA-NPs on the photosynthetic activity of *Chlorella*, the chlorophyll fluorescence parameters were examined. The results showed that the maximum quantum efficiency ( $F_v/F_m$ ) of photosystem II was significantly reduced in 100  $\mu\text{g mL}^{-1}$  ECA-NP-treated cells compared to the control (Fig. 5D) ( $p \leq 0.01$ ), whereas the relative maximum electron transport rate (rETR) increased in the ECA-NP treated cells (Fig. 5E). These results indicated that the photochemical activity was repressed, and occurrence of photoinhibition was

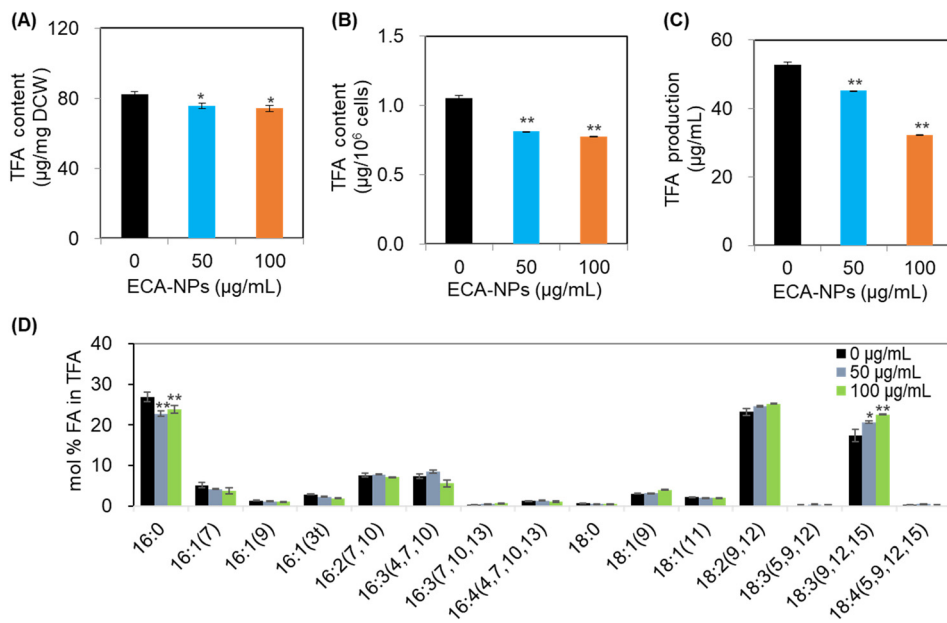


**Fig. 4** The content and profile of TFA in *Chlorella vulgaris* treated with ECA-NPs. (A–C) TFA content and production of the cells following exposure to different concentrations of ECA-NPs, respectively. TFA, total fatty acids; DCW, dry cell weight. (D) Fatty acid (FA) composition of TFA. Values are shown as mol% of total FAs. The cells were collected for analysis following a three-day treatment with ECA-NPs. Statistical analysis was conducted using Student's *t*-test (\**p* ≤ 0.05, \*\**p* ≤ 0.01).

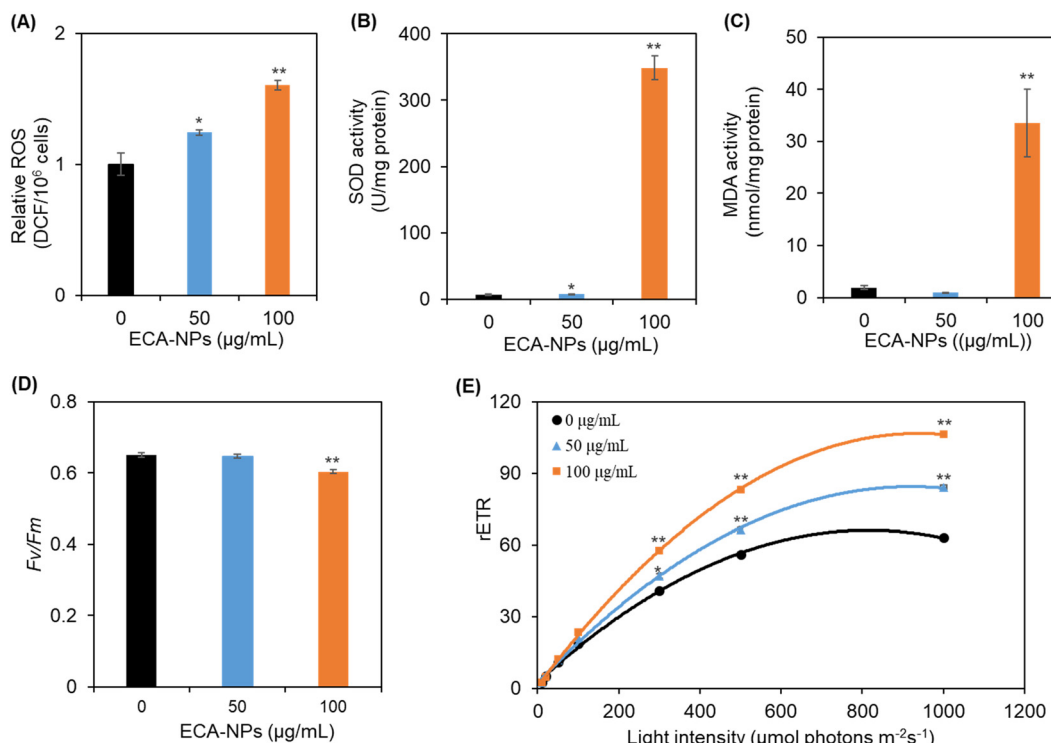


**Fig. 5** The oxidative stress and photosynthetic activity in *Chlorella vulgaris* treated with ECA-NPs. (A) The content of reactive oxygen species (ROS) in the cells following exposure to different concentrations of ECA-NPs. (B and C) The activities of antioxidant enzymes. SOD, superoxide dismutase; MDA, malondialdehyde. (D and E) The changes of chlorophyll fluorescence parameters.  $F_v/F_m$ , the maximum quantum efficiency of photosystem II; rETR, the relative maximum electron transport rate. The cells were harvested for analysis after a three-day ECA-NP treatment. Statistical analysis was conducted using Student's *t*-test (\**p* ≤ 0.05, \*\**p* ≤ 0.01).

inevitable. The increase of rETR in ECA-NP treated cells suggested the potential increase of photosynthetic electron transport.

### Transcriptome analysis after exposure to ECA-NPs

To detect the metabolic pathways and explore the transcriptional responses that were significantly affected by the exposure to ECA-NPs, transcriptome analysis was carried out. A total of 4652 genes were identified for *Chlorella*, of which 1335 genes were significantly upregulated and 3210 genes were downregulated ( $\log_2$ FC value  $\geq 1$ ) in comparison with the untreated cells (Fig. 6A) (ESI† data file1). The gene ontology (GO) enrichment analysis showed that differentially expressed genes (DEGs) were primarily enriched in drug binding/catabolic process, chitin binding/metabolic process and carbohydrate derivative binding/metabolic process, suggesting that these biological processes were susceptible to be changed in *Chlorella* after ECA-NPs exposure (Fig. 6B) (ESI† data file2). The DEGs involved in regulation of apoptotic process, lipid transport/localization, hydrolase activity of glycosyl compounds/bonds, chitin binding/catabolic process and chitinase activity are highly enriched (Fig. 6B). Among the DEGs, the genes involved in drug binding/catabolic process, chemical stimulus detection, chitin binding/catabolic process and chitinase activity, glucosamine metabolic/catabolic process, and hydrolase activity of glycosyl compounds/bonds were downregulated in the ECA-NP-treated cells (Fig. S2A) (ESI† data file3), which may indicate a reduced capacity for their breakdown and utilization of these substances. This could indicate a potential response of ECA-NP-treated cells to environmental stressors that may affect their growth and survival. The genes involved in the membrane-bounded organelle, photosynthetic membrane and plastid thylakoid were upregulated (Fig. S2B) (ESI† data file4), which may indicate that the ECA-NP-exposed cells are adapting to improve their photosynthetic efficiency and metabolic processes under stress conditions. KEGG (Kyoto Encyclopedia of Genes and Genomes) pathway classification analysis suggested that the numbers of the genes involved in biological metabolism, such as carbohydrate, lipid and energy metabolism were highly enriched (Fig. 6C) (ESI† data file5). Notably, among the DEGs related to drug binding identified in comparison to the untreated cells, 30 genes were downregulated and 10 genes were upregulated ( $\log_2$ FC value  $\geq 1$ ) (ESI† data file6). The gene TRINITY\_DN2900\_c3\_g4 (Gene Sequencing ID) exhibited the most significant change (7-fold downregulation), will be investigated further in future studies to verify its biological function. These results could reflect a strategic shift in ECA-NP-treated cells aimed at optimizing energy metabolism to potentially improve their survival and resilience under stress conditions.

## Discussion

We previously reported that ECA-NPs exhibit antibacterial activity against various bacterial species. However, the effects of ECA-NPs on microalgae, which are primary producers in aquatic

ecosystems, remain unexplored. In this study, we found that high concentrations of ECA-NPs significantly inhibit the growth of *Chlorella*. TEM observation indicated that the internalization of ECA-NPs was accompanied by thinner cell walls, stacked thylakoid structures, and plasmolysis. ECA-NP exposure led to decreased total fatty acids and starch content, as well as reduced photosynthetic activity, while the EPS externalization, ROS generation and oil accumulation increased compared to the controls. Transcriptomic analysis revealed downregulation of genes related to drug binding and catabolic processes was observed, while genes associated with photosynthetic membranes and plastid thylakoids were upregulated. To the best of our knowledge, this is the first study to investigate toxicity mechanisms of ECA-NPs on microalgae, providing new insights into the impact on metabolic systems.

We previously found ECA-NPs exhibited the highest growth inhibitory effects against all examined bacterial species among the resin nanoparticles tested, indicating their strong antibacterial effect. In addition, ECA-NPs exhibited a greater inhibitory effect on Gram-positive bacteria (e.g., *B. subtilis*) compared to Gram-negative bacteria (e.g., *E. coli*).<sup>17</sup> The differences in cell wall structure between Gram-positive and Gram-negative bacteria likely contribute to their varying susceptibility to ECA-NPs. Gram-negative bacteria possess an additional outer membrane outside the peptidoglycan layer,<sup>29,30</sup> which may act as an effective barrier to block the penetration of external molecules like ECA-NPs. In contrast, the simpler cell wall structure of Gram-positive bacteria, consisting primarily of peptidoglycan,<sup>29</sup> may allow for easier access and interaction of ECA-NPs, leading to enhanced antimicrobial activity of ECA-NPs against these species, since the composition of polysaccharides in the cell wall and the specific arrangement of cell wall proteins may significantly influence the nature and severity of subsequent metabolic abnormalities.

The cell walls of *Chlorella* are composed of a rigid, single-layered microfibrillar structure primarily made up of chitin- or chitosan-like polysaccharides rather than cellulose fibers.<sup>31,32</sup> Our results showed that high concentrations of ECA-NPs are toxic to *Chlorella* (Fig. 1A), likely due to the internalization of ECA-NPs through damages of the cell wall, as observed through TEM (Fig. 1B). ECA-NPs were prominently observed in the periplasmic space and vacuoles in the ECA-NP-exposed *Chlorella* (Fig. 1B and S1†). The internalization of NPs was also found in metallic oxide NP (e.g.,  $\text{TiO}_2$ ) and other cyanoacrylate resin NP (e.g., iBCA-NPs) treated microalgae, such as *Chlorella pyrenoidosa* and *Chlamydomonas reinhardtii* (thereafter *Chlamydomonas*).<sup>18,33</sup> In iBCA-NP-exposed *Chlamydomonas*, the particles also accumulated in the periplasmic space and vacuoles, with iBCA-NP surrounded by a membrane-like structure of uncertain origin.<sup>18</sup> However, in ECA-NP-treated *Chlorella*, such a membrane-like structure was not observed, suggesting that microalgae respond differently to various NPs. After exposure to ECA-NPs, the cells exhibited stacked thylakoid structures (Fig. 1B), which may indicate damage to photosynthetic activity. Indeed, we found that ECA-NP-exposed



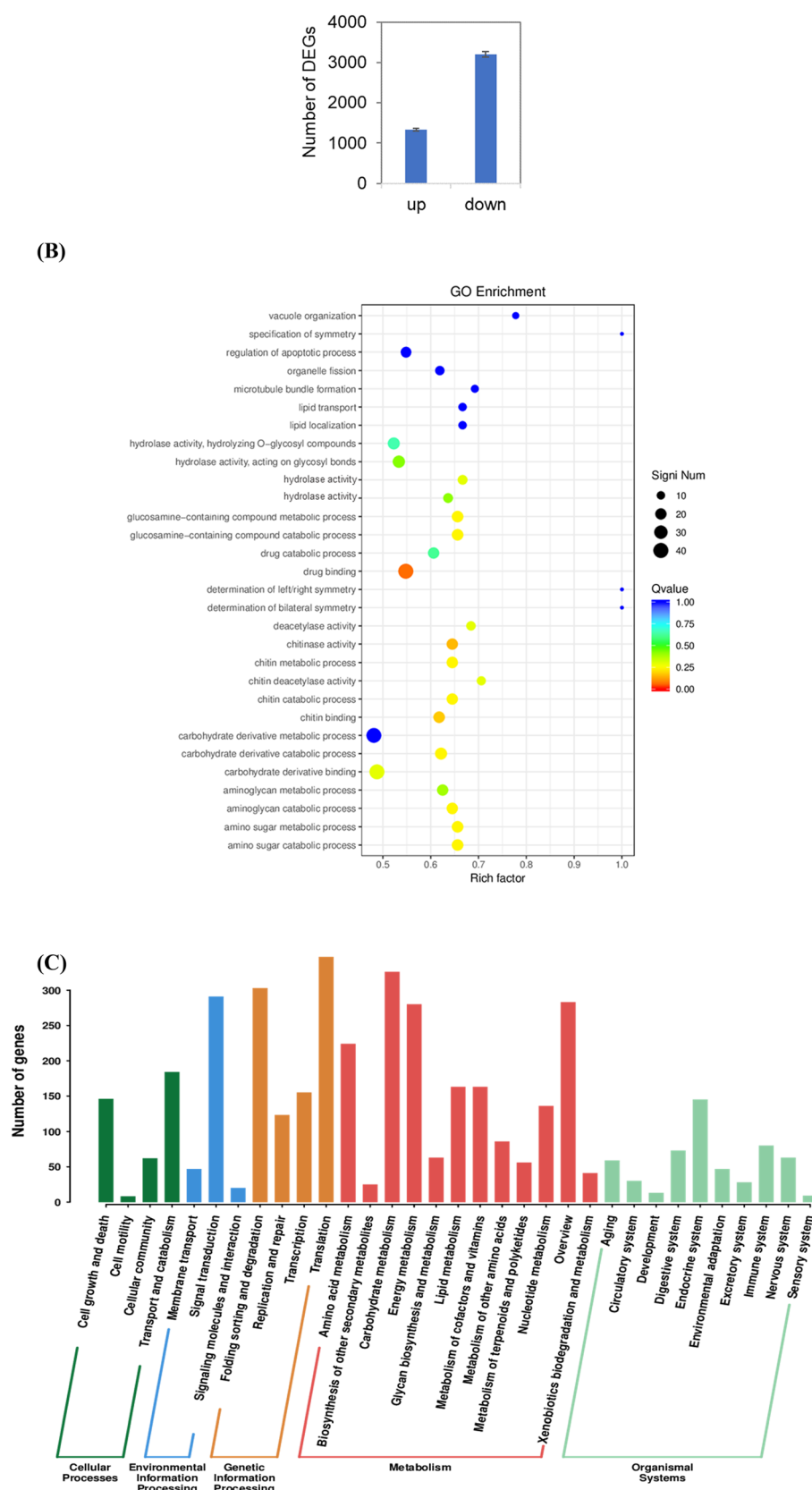


**Fig. 6** Transcriptional response of *Chlorella vulgaris* exposed to ECA-NPs. (A) Number of differentially expressed genes (DEGs) calculated with fold change (ECA-NP exposure/ECA-NP free)  $\geq 1$  and FDR-corrected  $P$ -value  $\leq 0.05$ . (B) Biological process GO enrichment of the DEGs. (C) KEGG pathway classification of the DEGs. The cells were harvested for analysis after three-day ECA-NP treatment.

cells exhibited lower  $F_v/F_m$  and showed increased ROS generation and higher activities of antioxidant enzymes (e.g., SOD and MDA) (Fig. 5A–C). The interplay between ROS levels and antioxidant defense mechanisms dictates the onset and severity of oxidative stress response and cellular damage.<sup>34</sup> The elevated ROS levels are likely to cause oxidative damage in microalgae.<sup>35</sup> Therefore, our results indicated that oxidative stress induced by ECA-NPs may surpass the scavenging capacity of cellular antioxidant defenses, leading to oxidative damage and inhibited cell growth of *Chlorella*.

Extracellular polymeric substances (EPS) are regarded as crucial self-defense in *Chlorella* against exogenous stimuli.<sup>27</sup> Meanwhile, enhanced secretion of EPS in response to NP exposure is regarded as a significant feedback mechanism for microalgae.<sup>36</sup> Our results indicated that the EPS content in *Chlorella* was significantly higher under ECA-NP exposure (Fig. 2). Similarly, Zhu *et al.* reported that increasing concentrations of  $TiO_2$  NPs significantly inhibit EPS secretion by *Chlorella pyrenoidosa*.<sup>33</sup> This antagonistic effect allows more  $TiO_2$  NPs to penetrate into the algal cells. Furthermore, it was reported that weakened EPS protection of algal cells is the primary mechanism behind the enhanced toxicity of  $TiO_2$  NPs.<sup>33</sup> Therefore, the increased EPS production following ECA-NP treatment is triggered by the internalization of ECA-NPs, which may be attributed to the enhanced ROS generation,<sup>37</sup> as significantly elevated ROS levels are responsible for the increased EPS secretion in microalgae following exposure to metallic oxide NPs.<sup>33</sup>

Triacylglycerol (TAG) biosynthesis in microalgae is a crucial response to stress conditions, such as nutrient limitation and environmental pollutants.<sup>38</sup> Under stress conditions, microalgae often redirect their metabolic pathways to accumulate TAGs as an energy reserve, which serves as a protective mechanism against adverse conditions.<sup>39</sup> Our results indicated that exposure to ECA-NPs enhanced triacylglycerol (TAG) accumulation and production in *Chlorella vulgaris* (Fig. 3A–C). Similar effects were also observed in a previous report demonstrating increased TAG content in *Chlamydomonas* cells treated with iBCA-NPs.<sup>20</sup> The synthesis of TAGs is facilitated by the upregulation of specific enzymes involved in energy metabolism, allowing microalgae to convert excess carbohydrates and fatty acids into storage oils (mainly TAGs).<sup>40,41</sup> This could be one of the reasons for the reduced starch accumulation in ECA-NP treated *Chlorella vulgaris* (Fig. 3D–F), as previous studies have indicated blocking starch synthesis could increase TAG content in microalgae.<sup>42–44</sup> Starch serves as another major carbon reservoir in green microalgae. Shunting carbon precursors from the starch synthesis pathway may lead to an overproduction of fatty acids, consequently resulting in increased TAG accumulation.<sup>45</sup> TAG accumulation not only provides a source of energy for cellular processes during the stress phase, but also enhances the resilience of microalgae to oxidative damage.<sup>46</sup>

We previously found that in *Chlamydomonas* cells treated with iBCA-NPs, the expression levels of heat shock proteins, ROS detoxification enzymes, and cell wall hydrolytic enzymes

were significantly upregulated as a response to the stresses induced by ROS accumulation.<sup>47</sup> In the *Chlorella pyrenoidosa* cells treated with metallic oxide  $TiO_2$ -NPs, the genes associated with the  $Ca^{2+}$  signaling pathway, biological synthesis, and protein metabolism were upregulated.<sup>37</sup> This upregulation is considered to contribute to increased ROS generation, which in turn leads to enhanced EPS secretion in response to the stress caused by  $TiO_2$ -NP exposure.<sup>37</sup> In this study, our results showed that the genes involved in the drug binding and catabolic process, chemical stimulus detection, chitin binding and catabolic process, chitinase activity, glucosamine metabolic and catabolic process, and hydrolase activity of glycosyl compounds and bonds were downregulated in the ECA-NP-treated cells (Fig. S2A†). *Chlorella* species are classified into two groups based on their cell wall composition: the glucose–mannose type and the glucosamine type. *C. vulgaris* and *C. sorokiniana* (true-*Chlorella*).<sup>48</sup> The true-*Chlorella* are characterized by glucosamine as the predominant component of their rigid walls, along with galactose and rhamnose. It is generally believed that the cell wall of true-*Chlorella* consists of a microfibrillar single-layered structure made of chitin- or chitosan-like polysaccharides instead of cellulose fibers.<sup>31,32,49</sup> The downregulation of genes involved in chitin binding and catabolic processes, and glucosamine metabolic and catabolic processes, along with reduced chitinase activity, may act as a feedback response to ECA-NP exposure to maintain cell wall integrity and reduce ECA-NP internalization. Additionally, the downregulation of genes related to chemical stimulus detection and drug binding/catabolic processes likely serves as a feedback mechanism to minimize ECA-NP uptake and mitigate cytotoxicity. Meanwhile, the genes associated with membrane-bounded organelles, photosynthetic membranes and plastid thylakoids were upregulated (Fig. S2B†). These results indicated that the ECA-NP-exposed cells are adapting to recover their photosynthetic efficiency, which may improve their survival and resilience under stress conditions. Our study revealed that the microalga *Chlorella vulgaris* responds to ECA-NPs through a distinct mechanism compared to those previous studies. The varying responses to ECA-NPs among different species may be due to that they effect the entire regulation of metabolic pathways, some of which are unique or characteristic to individual species.

## Conclusions

ECA-NPs treatment wreaked the cell wall structure of *Chlorella vulgaris*, and the internalization of ECA-NPs caused damages to organelles, particularly the chloroplasts. In the ECA-NP treated cells, the photosynthetic activity was decreased, whereas ROS generation was increased. Moreover, the EPS and TAG production were also enhanced. Transcriptomic analysis indicated that the genes that are involved in the drug binding/catabolic process and cell wall component catabolic process (chitin catabolism), while genes involved in photosynthetic membrane and plastid thylakoid were upregulated. This study



proposed a possible mechanism of microalgae in response to novel antibacterial ethyl cyanoacrylate nanoparticles.

## Materials and methods

### Strains and culture conditions

*Chlorella vulgaris* FACHB-31, used in this study, was purchased from Freshwater Algae Culture Collection at the Institute of Hydrobiology, Chinese Academy of Sciences (Wuhan, China). The strain was cultivated in BG-11 medium<sup>50</sup> as previously described. *Chlorella* was inoculated in 40 mL of BG-11 medium in 200 ml Erlenmeyer flasks (20%, v/v). Unless otherwise stated, the flasks were incubated at 25 °C under constant cool-white fluorescent light illumination (50  $\mu\text{mol m}^{-2} \text{ s}^{-1}$ ) with gentle shaking. Algal cells at the exponential phase were used for experimental setups.

### ECA-NP synthesis and exposure experiments

The ECA-NPs were synthesized *via* emulsion polymerization using Tween 80 as a surfactant as we previously described.<sup>17</sup> Briefly, commercially available cyanoacrylate monomers (Aron Alpha 201, Aichi, Japan) were added dropwise into 5 N HCl containing 4% (v/v) Tween 80. The monomer addition continued until it reached 4% (v/v) of the HCl solution. The mixture was stirred continuously (250 rpm) at 25 °C. After stirring for 2 h to aggregate the polymer particles, 0.5 N sodium hydroxide (NaOH) was added dropwise until the pH reached 7.0. The solution was stirred for an additional hour to generate solid nanoparticles. The size distribution and zeta potential of the synthesized ECA-NPs were immediately measured using a zeta-potential & particle size analyzer (ELSZ-2000ZS, Otsuka Electronics, Japan). The solution was filtered using a 5  $\mu\text{m}$  pore size membrane filter to remove any debris and stored at 4 °C until further use. Algal cells in the exponential phase ( $2 \times 10^6$  cells per mL) were treated with 50, 100, and 200  $\mu\text{g mL}^{-1}$  of ECA-NPs, respectively. The control group consisted of 0  $\mu\text{g mL}^{-1}$  ECA-NPs, supplemented with the same amount of surfactant used to prepare the ECA-NPs. Cell numbers were measured using an automated Algae Counter (Countstar BioMarine).

### Transmission electron microscopy observations

Transmission electron microscopy (TEM) was conducted as we previously described with modifications.<sup>18,51</sup> Briefly, cells exposed to 100  $\mu\text{g mL}^{-1}$  ECA-NPs for three days were collected by centrifugation at 1500 rpm for 3 min at 25 °C. The samples were washed twice with 1× PBS and fixed in 2.5% glutaraldehyde (pH 7.4) for 4 h. They were then washed with 0.1 M phosphate buffer (pH 7.2) and fixed in 1% osmic acid at 4 °C for 2 h. The samples were then subjected to gradient dehydration through a series of ethanol solutions. Subsequently, they were embedded in Epon-Araldite resin for penetration and placed in a mold for polymerization. Ultrathin sections of well-fixed cells were prepared and stained with both 3% uranyl acetate for 5 min followed by

2.7% lead citrate for 10 min at 25 °C. The ultrathin sections were observed under a HT7800 transmission electron microscope (Hitachi, Japan).

### EPS extraction and measurement

EPS were extracted and quantified following the method described previously.<sup>52</sup> Briefly, 10 mL of algal culture was heated at 45 °C for 30 min, followed by centrifugation at 3500 rpm for 5 minutes. The supernatant was collected and filtered using a 0.45  $\mu\text{m}$  membrane filters. The anthrone-sulfuric acid method<sup>53</sup> and Bradford method<sup>54</sup> were utilized for quantifying of polysaccharides and proteins in the EPS, respectively, as we previously described.<sup>55,56</sup> Commercial glucose and bovine serum albumin (Takara, Japan) were used to create the standard curves. The EPS content was calculated based on the total concentration of polysaccharides and proteins as previously described.<sup>52</sup>

### Starch and lipid analysis

Total starch was quantified using the anthrone-sulfuric acid colorimetry method as previously described.<sup>56</sup> Briefly, the cell cultures were harvested and resuspended in 1.0 mL of 80% ethanol (v/v). The suspension was then autoclaved at 120 °C for 15 min. Following enzymic hydrolysis of starch by amyloglucosidase (1.5 U) at 55 °C for 2 h, 150  $\mu\text{L}$  of the anthrone chemical agent was supplemented. The mixture was incubated at 100 °C for 10 min and subsequently measured at 621 nm using spectrophotometry (TECAN, Infinite 200 PRO).

Total lipids from algal samples were extracted using the Bligh and Dyer method with modifications.<sup>57,58</sup> The extracted lipids were dried and then dissolved in a mixture of chloroform : methanol (2 : 1, v/v) for thin-layer chromatography (TLC) analysis. TAGs were separated on TLC plates (Merck) by a solvent mixture of hexanediethyl ether-acetic acid (85 : 15 : 1, v/v/v) and subsequently recovered. Total lipids and recovered TAGs were transmethylated into fatty acid methyl esters (FAMEs) through a direct transmethylation method. FAMEs were quantified using gas chromatography with a flame ionization detector (GC-FID) according to our previously described procedures.<sup>20,59</sup>

### ROS accumulation detection

The reactive oxygen species (ROS) levels were determined using a ROS assay kit (Beyotime) as previously reported.<sup>20,60</sup> Briefly, cells in the exponential growth phase were collected (20 million cells) by centrifugation and washed twice with PBS. The cells were resuspended in 100  $\mu\text{L}$  fresh PBS buffer containing 10  $\mu\text{M}$  fluorogenic probe 2',7'-dichlorodihydrofluorescein diacetate (DCFH-DA). The samples were incubated at 37 °C in the dark for 30 minutes. After incubation, the fluorescence intensity was measured using a fluorescence microplate reader with excitation at 488 nm and emission at 525 nm. A standard curve using H<sub>2</sub>O<sub>2</sub> solutions of known concentrations was prepared to



quantify the ROS levels. ROS levels in the samples were calculated based on the standard curve.

### Antioxidant enzyme activity analysis

The activities of superoxide dismutase (SOD) and malondialdehyde (MDA) were measured using colorimetric assay kits (Acmeec Biochemical) according to the manufacturer's instructions, respectively. Briefly, cells in the logarithm phase were collected and resuspended in an extraction buffer, and then lysed by sonication. For SOD activity measurement, the reaction mixture was incubated at 25 °C for 10 min and the absorbance of each sample was measured at 560 nm. For MDA activity measurement, the samples were incubated at 100 °C for 60 min, and then cooled down. After centrifuging at 10 000g for 10 min at 25 °C, the supernatant was used for absorbance measurements at 450 nm, 532 nm, and 600 nm, respectively. The protein contents of samples were determined using a bicinchoninic acid (BCA) protein assay kit (Takara), and the enzyme activity was calculated as units per micrograms of protein according to the manufacturer's instructions, respectively.

### Photosynthetic characteristics measurement

The cells in the exponential growth phase were utilized and diluted to an appropriate concentration if needed to ensure accurate measurements. The samples were incubated in the dark for 10 minutes to allow for full dark adaptation. Maximum quantum yield of PSII ( $F_v/F_m$ ) and relative maximum electron transport rate (rETR) were measured using a pulse-amplitude modulated fluorometry (Water-PAM, Germany) as we previously described.<sup>55,59</sup>

### Transcriptome analysis

The total RNA extraction, cDNA library preparation and RNA-seq were conducted by Sangon Biotech (Shanghai, China). Briefly, total RNA was isolated from the cells after three-day ECA-NP treatment using a total RNA extractor (Trizol). The integrity of the extracted RNA was examined with a Qubit2.0 fluorescence meter (Invitrogen) and gel electrophoresis. The cDNA library was prepared using a cDNA Synthesis Kit (Thermo) according to the manual. The sequences were analyzed using an Illumina HiSeq 2500. FastQC was utilized to conduct quality control on the raw data. The trimmed reads were aligned to the reference using Bowtie2. The reads mapped to the gene regions of the reference sequence were counted using Read Count v2.0.0. The level of mRNA expression was normalized by transcripts per million (TPM), and the differences were determined and are reported as log 2-fold changes. Functional enrichment analyses to determine the main biological functions and physiological metabolic pathway was performed using the Gene Ontology (GO) and Kyoto Encyclopedia of Genes and Genomes (KEGG).

### Statistical analysis

All the experiments were performed at least three times. Cell samples were collected from three independent cultures to obtain statistically data. The statistical significance of the differences was evaluated by Student's *t*-test using SPSS 18.0.

### Data availability

The data that support the findings of this study are available from the corresponding author upon reasonable request.

### Author contributions

Di Zhang: resources; data curation; formal analysis; visualization. Keqing Liu: investigation; resources; data curation; formal analysis. Chengcheng Feng: methodology; formal analysis, validation. Xianmin Wang: methodology; validation. Ayat J. S. Al-Azab: resources; methodology. Han Lu: methodology; validation. Haiyan Ma: resources; methodology. Ying Tang: resources; methodology. Li Xu: methodology. Takeshi Ohama: funding acquisition; project administration; writing-review & editing. Fantao Kong: conceptualization; data curation; formal analysis; investigation; methodology; funding acquisition; writing-original draft; writing-review & editing.

### Conflicts of interest

The authors declare no competing financial interest.

### Acknowledgements

This work was supported by the Natural Science Foundation of Liaoning Province of China (2024-MSLH-062), the Fundamental Research Funds for the Central Universities (DUT24BK033), and the Open Foundation of Key Laboratory of Industrial Ecology and Environmental Engineering, MOE [grant number KLEEE-23-02]. The authors acknowledged the assistance of the DUT Core Facilities of School of Bioengineering and Lingling Zheng from the Institute of Hydrobiology, Chinese Academy of Sciences, for the assistance of maintaining the *Chlorella vulgaris* strain.

### References

1. I. Chopra and M. Roberts, *Tetracycline Antibiotics: Mode of Action, Applications, Molecular Biology, and Epidemiology of Bacterial Resistance*, *Microbiol. Mol. Biol. Rev.*, 2001, **65**(2), 232–260, DOI: [10.1128/MMBR.65.2.232-260.2001](https://doi.org/10.1128/MMBR.65.2.232-260.2001).
2. A. A. Khan, K. N. Manzoor, A. Sultan, M. Saeed, M. Rafique, S. Noushad, A. Talib, S. Rentschler and H.-P. Deigner, Pulling the Brakes on Fast and Furious Multiple Drug-Resistant (MDR) Bacteria, *Int. J. Mol. Sci.*, 2021, **22**(2), 859, DOI: [10.3390/ijms22020859](https://doi.org/10.3390/ijms22020859).
3. D. Zheng, G. Yin, M. Liu, C. Chen, Y. Jiang, L. Hou and Y. Zheng, A Systematic Review of Antibiotics and Antibiotic Resistance Genes in Estuarine and Coastal Environments, *Sci. Total Environ.*, 2021, **777**, 146009, DOI: [10.1016/j.scitotenv.2021.146009](https://doi.org/10.1016/j.scitotenv.2021.146009).



4 A. K. Zeraatkar, H. Ahmadzadeh, A. F. Talebi, N. R. Moheimani and M. P. McHenry, Potential Use of Algae for Heavy Metal Bioremediation, a Critical Review, *J. Environ. Manage.*, 2016, **181**, 817–831, DOI: [10.1016/j.jenvman.2016.06.059](https://doi.org/10.1016/j.jenvman.2016.06.059).

5 F. Kong, C. Blot, K. Liu, M. Kim and Y. Li-Beisson, Advances in Algal Lipid Metabolism and Their Use to Improve Oil Content, *Curr. Opin. Biotechnol.*, 2024, **87**, 103130, DOI: [10.1016/j.copbio.2024.103130](https://doi.org/10.1016/j.copbio.2024.103130).

6 E. Nasoudari, M. Ameri, M. Shams, V. Ghavami and Z. Bonyadi, The Biosorption of Alizarin Red S by Spirulina Platensis; Process Modelling, Optimisation, Kinetic and Isotherm Studies, *Int. J. Environ. Anal. Chem.*, 2023, **103**(3), 633–647, DOI: [10.1080/03067319.2020.1862814](https://doi.org/10.1080/03067319.2020.1862814).

7 Z. Esmaili, B. Barikbin, M. Shams, H. Alidadi, T. J. Al-Musawi and Z. Bonyadi, Biosorption of Metronidazole Using Spirulina Platensis Microalgae: Process Modeling, Kinetic, Thermodynamic, and Isotherm Studies, *Appl. Water Sci.*, 2023, **13**(2), 63, DOI: [10.1007/s13201-023-01867-9](https://doi.org/10.1007/s13201-023-01867-9).

8 M. Eydi Gabrabad, M. Yari and Z. Bonyadi, Using Spirulina Platensis as a Natural Biocoagulant for Polystyrene Removal from Aqueous Medium: Performance, Optimization, and Modeling, *Sci. Rep.*, 2024, **14**(1), 2506, DOI: [10.1038/s41598-024-53123-y](https://doi.org/10.1038/s41598-024-53123-y).

9 C. Yu, H. Pang, J.-H. Wang, Z.-Y. Chi, Q. Zhang, F.-T. Kong, Y.-P. Xu, S.-Y. Li and J. Che, Occurrence of Antibiotics in Waters, Removal by Microalgae-Based Systems, and Their Toxicological Effects: A Review, *Sci. Total Environ.*, 2022, **813**, 151891, DOI: [10.1016/j.scitotenv.2021.151891](https://doi.org/10.1016/j.scitotenv.2021.151891).

10 S. Sharmin, M. M. Rahaman, C. Sarkar, O. Atolani, M. T. Islam and O. S. Adeyemi, Nanoparticles as Antimicrobial and Antiviral Agents: A Literature-Based Perspective Study, *Heliyon*, 2021, **7**(3), e06456, DOI: [10.1016/j.heliyon.2021.e06456](https://doi.org/10.1016/j.heliyon.2021.e06456).

11 M. Ahamed, M. S. Alsalhi and M. K. J. Siddiqui, Silver Nanoparticle Applications and Human Health, *Clin. Chim. Acta*, 2010, **411**(23–24), 1841–1848, DOI: [10.1016/j.cca.2010.08.016](https://doi.org/10.1016/j.cca.2010.08.016).

12 M. N. Ravi Kumar, Nano and Microparticles as Controlled Drug Delivery Devices, *J. Pharm. Pharm. Sci.*, 2000, **3**(2), 234–258.

13 C. Vauthier, C. Dubernet, E. Fattal, H. Pinto-Alphandary and P. Couvreur, Poly(Alkylcyanoacrylates) as Biodegradable Materials for Biomedical Applications, *Adv. Drug Delivery Rev.*, 2003, **55**(4), 519–548, DOI: [10.1016/s0169-409x\(03\)00041-3](https://doi.org/10.1016/s0169-409x(03)00041-3).

14 E. Sulheim, H. Baghirov, E. von Haartman, A. Bøe, A. K. O. Åslund, Y. Mørch and C. de L. Davies, Cellular Uptake and Intracellular Degradation of Poly(Alkyl Cyanoacrylate) Nanoparticles, *J. Nanobiotechnol.*, 2016, **14**, 1, DOI: [10.1186/s12951-015-0156-7](https://doi.org/10.1186/s12951-015-0156-7).

15 J. M. Korde and B. Kandasubramanian, Biocompatible Alkyl Cyanoacrylates and Their Derivatives as Bio-Adhesives, *Biomater. Sci.*, 2018, **6**(7), 1691–1711, DOI: [10.1039/c8bm00312b](https://doi.org/10.1039/c8bm00312b).

16 R. Y. Pelgrift and A. J. Friedman, Nanotechnology as a Therapeutic Tool to Combat Microbial Resistance, *Adv. Drug Delivery Rev.*, 2013, **65**(13–14), 1803–1815, DOI: [10.1016/j.addr.2013.07.011](https://doi.org/10.1016/j.addr.2013.07.011).

17 F. D. Sarian, K. Ando, S. Tsurumi, R. Miyashita, K. Ute and T. Ohama, Evaluation of the Growth-Inhibitory Spectrum of Three Types of Cyanoacrylate Nanoparticles on Gram-Positive and Gram-Negative Bacteria, *Membranes*, 2022, **12**(8), 782, DOI: [10.3390/membranes12080782](https://doi.org/10.3390/membranes12080782).

18 D. Widyaningrum, D. Iida, Y. Tanabe, Y. Hayashi, S. D. Kurniasih and T. Ohama, Acutely Induced Cell Mortality in the Unicellular Green Alga Chlamydomonas Reinhardtii (Chlorophyceae) Following Exposure to Acrylic Resin Nanoparticles, *J. Phycol.*, 2019, **55**(1), 118–133, DOI: [10.1111/jpy.12798](https://doi.org/10.1111/jpy.12798).

19 A. J. S. Al-Azab, D. Widyaningrum, H. Hirakawa, Y. Hayashi, S. Tanaka and T. Ohama, A Resin Cyanoacrylate Nanoparticle as an Acute Cell Death Inducer to Broad Spectrum of Microalgae, *Algal Res.*, 2021, **54**, 102191, DOI: [10.1016/j.algal.2021.102191](https://doi.org/10.1016/j.algal.2021.102191).

20 H. Lu, K. Liu, H. Zhang, X. Xie, Y. Ge, Z. Chi, S. Xue, F. Kong and T. Ohama, Enhanced Triacylglycerols and Starch Synthesis in Chlamydomonas Stimulated by the Engineered Biodegradable Nanoparticles, *Appl. Microbiol. Biotechnol.*, 2023, **107**(2–3), 971–983, DOI: [10.1007/s00253-023-12366-x](https://doi.org/10.1007/s00253-023-12366-x).

21 F. D. Sarian and T. Ohama, Comparable Antibacterial Effects and Action Mechanisms of Ethyl Cyanoacrylate Nanoparticles on *Bacillus Subtilis* and *Escherichia Coli* Evaluated by Transcriptome and Morphological Changes, *Environ. Sci.: Nano*, 2023, **10**(7), 1932–1941, DOI: [10.1039/D3EN00054K](https://doi.org/10.1039/D3EN00054K).

22 F. Barari, M. Eydi Gabrabad and Z. Bonyadi, Recent Progress on the Toxic Effects of Microplastics on Chlorella Sp. in Aquatic Environments, *Heliyon*, 2024, **10**(12), e32881, DOI: [10.1016/j.heliyon.2024.e32881](https://doi.org/10.1016/j.heliyon.2024.e32881).

23 M. Z. Anbarani, B. Ramavandi and Z. Bonyadi, Modification of Chlorella Vulgaris Carbon with Fe3O4 Nanoparticles for Tetracycline Elimination from Aqueous Media, *Heliyon*, 2023, **9**(3), e14356, DOI: [10.1016/j.heliyon.2023.e14356](https://doi.org/10.1016/j.heliyon.2023.e14356).

24 J. Liu and F. Chen, Biology and Industrial Applications of Chlorella: Advances and Prospects, in *Microalgae Biotechnology*, ed. C. Posten and S. Feng Chen, Springer International Publishing, Cham, 2016, pp. 1–35, DOI: [10.1007/10\\_2014\\_286](https://doi.org/10.1007/10_2014_286).

25 H. Rafeeq, N. Afsheen, S. Rafique, A. Arshad, M. Intisar, A. Hussain, M. Bilal and H. M. N. Iqbal, Genetically Engineered Microorganisms for Environmental Remediation, *Chemosphere*, 2023, **310**, 136751, DOI: [10.1016/j.chemosphere.2022.136751](https://doi.org/10.1016/j.chemosphere.2022.136751).

26 S. M. Aly, N. I. ElBanna and M. Fathi, Chlorella in Aquaculture: Challenges, Opportunities, and Disease Prevention for Sustainable Development, *Aquacult. Int.*, 2024, **32**(2), 1559–1586, DOI: [10.1007/s10499-023-01229-x](https://doi.org/10.1007/s10499-023-01229-x).

27 R. Xiao and Y. Zheng, Overview of Microalgal Extracellular Polymeric Substances (EPS) and Their Applications, *Biotechnol. Adv.*, 2016, **34**(7), 1225–1244, DOI: [10.1016/j.biotechadv.2016.08.004](https://doi.org/10.1016/j.biotechadv.2016.08.004).

28 M. Vitova, K. Bisova, S. Kawano and V. Zachleder, Accumulation of Energy Reserves in Algae: From Cell Cycles to Biotechnological Applications, *Biotechnol. Adv.*, 2015, **33**(6 Pt 2), 1204–1218, DOI: [10.1016/j.biotechadv.2015.04.012](https://doi.org/10.1016/j.biotechadv.2015.04.012).



29 C. Kleanthous and J. P. Armitage, The Bacterial Cell Envelope, *Philos. Trans. R. Soc., B*, 2015, **370**(1679), 20150019, DOI: [10.1098/rstb.2015.0019](https://doi.org/10.1098/rstb.2015.0019).

30 T. Dörr, P. J. Moynihan and C. Mayer, Editorial: Bacterial Cell Wall Structure and Dynamics, *Front. Microbiol.*, 2019, **10**, 2051, DOI: [10.3389/fmicb.2019.02051](https://doi.org/10.3389/fmicb.2019.02051).

31 S. Weber, P. M. Grande, L. M. Blank and H. Klose, Insights into Cell Wall Disintegration of Chlorella Vulgaris, *PLoS One*, 2022, **17**(1), e0262500, DOI: [10.1371/journal.pone.0262500](https://doi.org/10.1371/journal.pone.0262500).

32 K. Brückner and C. Griechl, Permeabilization of the Cell Wall of Chlorella Sorokiniana by the Chitosan-Degrading Protease Papain, *Algal Res.*, 2023, **71**, 103066, DOI: [10.1016/j.algal.2023.103066](https://doi.org/10.1016/j.algal.2023.103066).

33 L. Zhu, A. M. Booth, S. Feng, C. Shang, H. Xiao, X. Tang, X. Sun, X. Zhao, B. Chen, K. Qu and B. Xia, UV-B Radiation Enhances the Toxicity of TiO<sub>2</sub> Nanoparticles to the Marine Microalga Chlorella Pyrenoidosa by Disrupting the Protection Function of Extracellular Polymeric Substances, *Environ. Sci.: Nano*, 2022, **9**(5), 1591–1604, DOI: [10.1039/DEN01198G](https://doi.org/10.1039/DEN01198G).

34 N. Mallick and F. H. Mohn, Reactive Oxygen Species: Response of Algal Cells, *J. Plant Physiol.*, 2000, **157**(2), 183–193, DOI: [10.1016/S0176-1617\(00\)80189-3](https://doi.org/10.1016/S0176-1617(00)80189-3).

35 M. K. Nguyen and H. M. Kim, A Review of the Representative Microalgal-Derived Reactive Oxygen Species: Possible Formation, Ecophysiological Implications, and Metabolomic-Based Evaluations, *J. Appl. Phycol.*, 2024, **36**(1), 129–154, DOI: [10.1007/s10811-023-03132-7](https://doi.org/10.1007/s10811-023-03132-7).

36 J. Hou, Y. Yang, P. Wang, C. Wang, L. Miao, X. Wang, B. Lv, G. You and Z. Liu, Effects of CeO<sub>2</sub>, CuO, and ZnO Nanoparticles on Physiological Features of *Microcystis Aeruginosa* and the Production and Composition of Extracellular Polymeric Substances, *Environ. Sci. Pollut. Res.*, 2017, **24**(1), 226–235, DOI: [10.1007/s11356-016-7387-5](https://doi.org/10.1007/s11356-016-7387-5).

37 X. Gao, R. Deng and D. Lin, Insights into the Regulation Mechanisms of Algal Extracellular Polymeric Substances Secretion upon the Exposures to Anatase and Rutile TiO<sub>2</sub> Nanoparticles, *Environ. Pollut.*, 2020, **263**, 114608, DOI: [10.1016/j.envpol.2020.114608](https://doi.org/10.1016/j.envpol.2020.114608).

38 Z.-Y. Du and C. Benning, Triacylglycerol Accumulation in Photosynthetic Cells in Plants and Algae, *Subcell. Biochem.*, 2016, **86**, 179–205, DOI: [10.1007/978-3-319-25979-6\\_8](https://doi.org/10.1007/978-3-319-25979-6_8).

39 Y. Li-Beisson, J. J. Thelen, E. Fedosejevs and J. L. Harwood, The Lipid Biochemistry of Eukaryotic Algae, *Prog. Lipid Res.*, 2019, **74**, 31–68, DOI: [10.1016/j.plipres.2019.01.003](https://doi.org/10.1016/j.plipres.2019.01.003).

40 F. Kong, I. T. Romero, J. Warakanont and Y. Li-Beisson, Lipid Catabolism in Microalgae, *New Phytol.*, 2018, **218**(4), 1340–1348, DOI: [10.1111/nph.15047](https://doi.org/10.1111/nph.15047).

41 Y. Li-Beisson, J. Warakanont, W. Riekhof and C. Benning, in *The Chlamydomonas Sourcebook*, ed. A. R. Grossman and F.-A. Wollman, Academic Press, London, 3rd edn, 2023, ch. 2 - Chlamydomonas Glycerolipid Metabolism, pp. 51–97, DOI: [10.1016/B978-0-12-821430-5.00009-2](https://doi.org/10.1016/B978-0-12-821430-5.00009-2).

42 Y. Li, D. Han, G. Hu, D. Dauphinee, M. Sommerfeld, S. Ball and Q. Hu, Chlamydomonas Starchless Mutant Defective in ADP-Glucose Pyrophosphorylase Hyper-Accumulates Triacylglycerol, *Metab. Eng.*, 2010, **12**(4), 387–391, DOI: [10.1016/j.ymben.2010.02.002](https://doi.org/10.1016/j.ymben.2010.02.002).

43 L. de Jaeger, R. E. Verbeek, R. B. Draaisma, D. E. Martens, J. Springer, G. Eggink and R. H. Wijffels, Superior Triacylglycerol (TAG) Accumulation in Starchless Mutants of *Scenedesmus Obliquus*: (I) Mutant Generation and Characterization, *Biotechnol. Biofuels*, 2014, **7**(1), 69, DOI: [10.1186/1754-6834-7-69](https://doi.org/10.1186/1754-6834-7-69).

44 T. Li, M. Gargouri, J. Feng, J.-J. Park, D. Gao, C. Miao, T. Dong, D. R. Gang and S. Chen, Regulation of Starch and Lipid Accumulation in a Microalga Chlorella Sorokiniana, *Bioresour. Technol.*, 2015, **180**, 250–257, DOI: [10.1016/j.biortech.2015.01.005](https://doi.org/10.1016/j.biortech.2015.01.005).

45 W. Ran, H. Wang, Y. Liu, M. Qi, Q. Xiang, C. Yao, Y. Zhang and X. Lan, Storage of Starch and Lipids in Microalgae: Biosynthesis and Manipulation by Nutrients, *Bioresour. Technol.*, 2019, **291**, 121894, DOI: [10.1016/j.biortech.2019.121894](https://doi.org/10.1016/j.biortech.2019.121894).

46 S. S. Merchant, J. Kropat, B. Liu, J. Shaw and J. Warakanont, TAG, You're It! Chlamydomonas as a Reference Organism for Understanding Algal Triacylglycerol Accumulation, *Curr. Opin. Biotechnol.*, 2012, **23**(3), 352–363, DOI: [10.1016/j.copbio.2011.12.001](https://doi.org/10.1016/j.copbio.2011.12.001).

47 A. J. S. Al-Azab, Y. Aoki, F. D. Sarian, Y. Sori, D. Widyaningrum, T. Yamasaki, F. Kong and T. Obama, Chronological Transcriptome Changes Induced by Exposure to Cyanoacrylate Resin Nanoparticles in Chlamydomonas Reinhardtii with a Focus on ROS Development and Cell Wall Lysis-Related Genes, *Algal Res.*, 2022, **68**, 102884, DOI: [10.1016/j.algal.2022.102884](https://doi.org/10.1016/j.algal.2022.102884).

48 H. Takeda, Taxonomical Assignment of Chlorococcal Algae from Their Cell Wall Composition, *Phytochemistry*, 1993, **34**(4), 1053–1055, DOI: [10.1016/S0031-9422\(00\)90712-X](https://doi.org/10.1016/S0031-9422(00)90712-X).

49 P.-H. Baudelet, G. Ricochon, M. Linder and L. Muniglia, A New Insight into Cell Walls of Chlorophyta, *Algal Res.*, 2017, **25**, 333–371, DOI: [10.1016/j.algal.2017.04.008](https://doi.org/10.1016/j.algal.2017.04.008).

50 Y. Feng, C. Li and D. Zhang, Lipid Production of Chlorella Vulgaris Cultured in Artificial Wastewater Medium, *Bioresour. Technol.*, 2011, **102**(1), 101–105, DOI: [10.1016/j.biortech.2010.06.016](https://doi.org/10.1016/j.biortech.2010.06.016).

51 H. Zhang, S. Ma, X. Dou, R. Chen, H. Lu, Z. Chi, S. Xue, Y. Li-Beisson and F. Kong, Harnessing Algal Peroxisomes for Efficient Poly Hydroxybutyrate Production, *ACS Sustainable Chem. Eng.*, 2024, **12**(8), 3312–3321, DOI: [10.1021/acssuschemeng.3c07974](https://doi.org/10.1021/acssuschemeng.3c07974).

52 Q. Wang, Q. Shen, J. Wang, J. Zhao, Z. Zhang, Z. Lei, T. Yuan, K. Shimizu, Y. Liu and D.-J. Lee, Insight into the Rapid Biogranulation for Suspended Single-Cell Microalgae Harvesting in Wastewater Treatment Systems: Focus on the Role of Extracellular Polymeric Substances, *Chem. Eng. J.*, 2022, **430**, 132631, DOI: [10.1016/j.cej.2021.132631](https://doi.org/10.1016/j.cej.2021.132631).

53 A. Leyva, A. Quintana, M. Sánchez, E. N. Rodríguez, J. Cremata and J. C. Sánchez, Rapid and Sensitive Anthrone-Sulfuric Acid Assay in Microplate Format to Quantify Carbohydrate in Biopharmaceutical Products: Method Development and Validation, *Biologicals*, 2008, **36**(2), 134–141, DOI: [10.1016/j.biologicals.2007.09.001](https://doi.org/10.1016/j.biologicals.2007.09.001).



54 N. J. Kruger, The Bradford Method For Protein Quantitation. in *The Protein Protocols Handbook*, ed. J. M. Walker, Humana Press, Totowa, NJ, 2009, pp. 17–24, DOI: [10.1007/978-1-59745-198-7\\_4](https://doi.org/10.1007/978-1-59745-198-7_4).

55 R. Chen, Y. Yamaoka, Y. Feng, Z. Chi, S. Xue and F. Kong, Co-Expression of Lipid Transporters Simultaneously Enhances Oil and Starch Accumulation in the Green Microalga Chlamydomonas Reinhardtii under Nitrogen Starvation, *Metabolites*, 2023, 13(1), 115, DOI: [10.3390/metabo13010115](https://doi.org/10.3390/metabo13010115).

56 J. Zhao, Y. Ge, K. Liu, Y. Yamaoka, D. Zhang, Z. Chi, M. Akkaya and F. Kong, Overexpression of a MYB1 Transcription Factor Enhances Triacylglycerol and Starch Accumulation and Biomass Production in the Green Microalga Chlamydomonas Reinhardtii, *J. Agric. Food Chem.*, 2023, 71(46), 17833–17841, DOI: [10.1021/acs.jafc.3c05290](https://doi.org/10.1021/acs.jafc.3c05290).

57 E. G. Bligh and W. J. Dyer, A Rapid Method of Total Lipid Extraction and Purification, *Can. J. Biochem. Physiol.*, 1959, 37(8), 911–917, DOI: [10.1139/o59-099](https://doi.org/10.1139/o59-099).

58 R. Chen, M. Yang, M. Li, H. Zhang, H. Lu, X. Dou, S. Feng, S. Xue, C. Zhu, Z. Chi and F. Kong, Enhanced Accumulation of Oil through Co-Expression of Fatty Acid and ABC Transporters in Chlamydomonas under Standard Growth Conditions, *Biotechnol. Biofuels Bioprod.*, 2022, 15(1), 54, DOI: [10.1186/s13068-022-02154-6](https://doi.org/10.1186/s13068-022-02154-6).

59 F. Kong, A. Burlacot, Y. Liang, B. Légeret, S. Alseekh, Y. Brotman, A. R. Fernie, A. Krieger-Liszakay, F. Beisson, G. Peltier and Y. Li-Beisson, Interorganelle Communication: Peroxisomal MALATE DEHYDROGENASE2 Connects Lipid Catabolism to Photosynthesis through Redox Coupling in Chlamydomonas, *Plant Cell*, 2018, 30(8), 1824–1847, DOI: [10.1105/tpc.18.00361](https://doi.org/10.1105/tpc.18.00361).

60 Y. Xi, F. Kong and Z. Chi, ROS Induce  $\beta$ -Carotene Biosynthesis Caused by Changes of Photosynthesis Efficiency and Energy Metabolism in Dunaliella Salina Under Stress Conditions, *Front. Bioeng. Biotechnol.*, 2021, 8, 1447, DOI: [10.3389/fbioe.2020.613768](https://doi.org/10.3389/fbioe.2020.613768).

